Simulation of broad spectral bandwidth emitters at 1060nm for optical coherence tomography

I G Tooley[1], D T D Childs[2], B J Stevens[1], K M Groom[1], R A Hogg[2],
[1] Department of Electronic and Electrical Engineering, University of Sheffield, Centre for Nanoscience & Technology, North Campus, Broad Lane, Sheffield, S3 7HQ, UK
[2] School of Engineering, Rankine Building, University of Glasgow, Glasgow, G12 8LT, UK

Abstract

The simulation of broad spectral bandwidth light sources (semiconductor optical amplifiers (SOA) and super-luminescent diodes (SLD)) for application in ophthalmic optical coherence tomography is reported. The device requirements and origin of key device parameters are outlined, and a range of single and double InGaAs/GaAs quantum well (QW) active elements are simulated with a view to application in different OCT embodiments. We confirm that utilising higher order optical transitions is beneficial for single QW SOAs, but may introduce deleterious spectral modulation in SLDs. We show how an addition QW may be introduced to eliminate this spectral modulation, but that this results in a reduction of the gain spectrum width. We go on to explore double QW structures where the roles of the two QWs are reversed, with the narrow QW providing long wavelength emission and gain. We show how this modification in the density of states results in a significant increase in gain-spectrum width for a given current.

Keywords: Device simulation, single quantum well, multi quantum well, density of states, time encoded frequency domain OCT, SOA, SLD

1. Introduction

Optical coherence tomography (OCT) of the eye is now a mature technology being first introduced in 1991 [1]. By using this technique it is possible to perform non-invasive, in-vivo three dimensional (3D) imaging of the retina with a resolution in the order of 3-15um and to a depth of around 2 millimetres. OCT is now commonly used to assist with the early diagnosis of eye diseases such as glaucoma, retinal pigmentosa and age related macular degeneration (wet and dry) [2]. Typical wavelengths employed are centred around ~800-900nm and use silicon based detectors. Marschall *et al*. [3] suggests that there is an advantage to using longer wavelengths centred on 1060nm to take advantage of a ~100nm dip in the absorption spectrum of the eye from 1010-1110nm. The particular benefits gained from using this waveband have been shown to be enhanced retinal penetration, improved visualisation beyond the retinal epithelium and reduced chromatic dispersion. There is therefore strong motivation to develop broad bandwidth, low cost, light sources to meet the needs of OCT. To deliver 1060nm wavelength the materials of choice are InGaAs/GaAs quantum wells.

OCT systems split into two main implementations, time domain OCT (TD-OCT) and frequency domain OCT (FD-OCT). In both of these systems light is split into a reference arm and a sample arm, with reflected light being recombined to produce interference patterns that can be analysed to produce a 3D image [4].

In TD-OCT systems the reference arm is moved in order to generate path length changes. Light from a broadband source (such as a super luminescent diode (SLD)) is used which is coherent over only a small spatial region governed by the coherence length, and hence the spectral bandwidth. An interference signal (envelope) is therefore observed only when the path length in the reference, and signal arms are equal. Changing the reference arm length therefore

interrogates a different depth of the sample being imaged. This type of OCT is a relatively slow process as time is required to translate the mirror.

In FD-OCT systems the mirror is fixed and a signal is acquired in the frequency domain. This is achieved by using spectrally resolved detection using a broadband source or by encoding the light wavelength in time with a spectrally scanning source. FD-OCT is comparatively faster at scanning as the reference mirror does not need to be moved, and enjoys a significant signal-to-noise advantage [5] over TD-OCT.

FD-OCT systems can thus be summarised into these two categories:

a) Time encoded frequency domain (swept source) TE-OCT [6] is where the spectral components are encoded in time by sweeping the wavelength of light. This type of system requires a broad bandwidth semiconductor amplifier (SOA)
b) Spatially encoded frequency domain (spectral domain or Fourier domain) SE-OCT extracts spectral information from all the different optical wavelengths using spectrally resolved detection. This type of system requires a broad bandwidth source such as an SLD

There are therefore two different devices required for OCT systems, the semiconductor optical amplifier (SOA) and the super-luminescent diode (SLD). In simple terms the spectral bandwidth of an SOA is governed by the gain spectrum of the device whilst the SLD spectrum is a convolution of the gain and the spontaneous emission spectra [7].

In this paper we will briefly outline the requirements of OCT in terms of broad band semiconductor devices. For the different embodiments of OCT, SOA's and SLD's are required. The operation of an SOA is essentially dominated by the gain spectrum whilst for an SLD the output power spectrum is governed by a convolution of gain and spontaneous emission spectrum. In this paper, we explore a range of single and double QW structures. We confirm that the use of higher order states broadens the gain spectrum, but in attempting to achieve broad band SLD's we show that this can result in significant undesirable spectral modulation. We describe how this SLD spectral modulation can be ameliorated by the introduction of an additional well for which the lowest energy optical transition is centred on the spectral dip. Having noted a reduction in the width of the gain spectrum in this case, we go on to explore "role reversal" QW's where the narrow QW has a high Indium concentration to achieve long wavelength emission. We show how the resultant modification to the DoS is beneficial in obtaining broad bandwidth gain for a given current density.

In order to simulate the modal gain and modal spontaneous emission we utilise a commercially available device simulation software suite of tools (LaserMod [8]), to simulate a range of parameters for single and multiple quantum well devices. The band structure is calculated using a 4x4 k.p model [9], the modal gain and spontaneous emission spectra are both generated by LaserMOD during the solving of the laser rate equations. All the devices simulated in this paper are a 3µm wide, 1000um long ridge and have a facet reflectivity at either end of $1x10^{-7}$. This device effective reflectivity R combines the effect of both angled facets [10], and AR coating of the facet. The epitaxial structure is composed of $Al_{(0.42)}Ga_{(0.58)}As$ cladding layers with a GaAs intrinsic region where the total thickness of the GaAs region plus all quantum wells has been maintained at a constant 135.2nm. The QW's are always centred on the middle of intrinsic region. By simulating and capturing the raw data from LaserMOD for modal gain and spontaneous emission data we were able to use this data to calculate the amplified spontaneous emission (ASE) using Equation 1.3 below.

The equation is derived by considering the small signal optical power change with respect to length of the SLD

Where P_0 is the spontaneous emission in the element *dz* and is linearly dependent on current density *J*

$$\frac{dP}{dz} = ßP + P_0$$

Equation (1.1)

Integration over the length of the device, L, gives

$$\frac{dP}{ßP+P_0} = \int_{z=0}^{L} 1.\,dz$$

Equation (1.2)

$$P = \frac{P_0}{ß}(e^{ßL} - 1)$$

Equation (1.3)

Where P is the ASE power out, P_0 is the spontaneous emission, ß is the gain

2. Results

With a target bandwidth of >100nm centred on 1060nm, we began by simulating a 4nm $In_{(0.3)}Ga_{(0.7)}As/GaAs$ single quantum well (SQW) device.

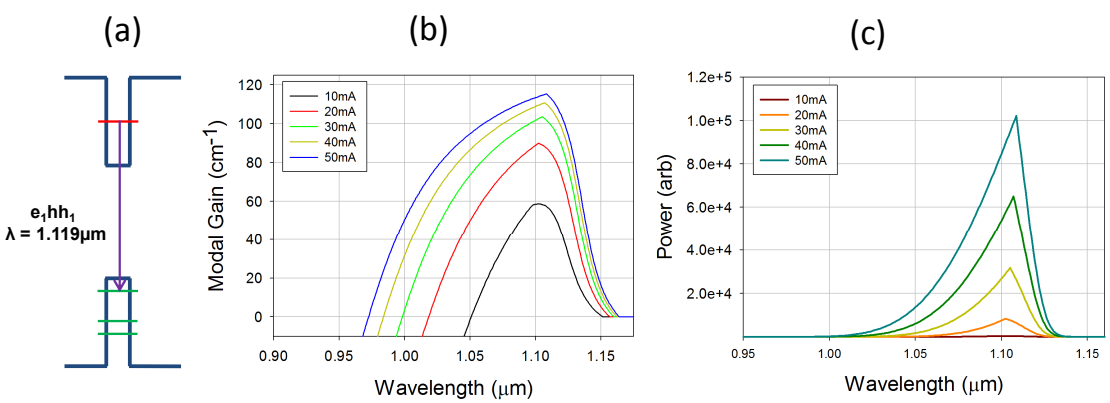

Figure 1 (a) band structure schematic of 4nm $In_{(0.3)}Ga_{(0.7)}As$ GaAs SQW device, (b) 4nm SQW device modal gain spectrum, (c) 4nm SQW device ASE power curve

Figure 1 (a) shows the schematic of the band structure of a 4nm $In_{(0.3)}Ga_{(0.7)}As$ SQW device (termed device A) has a ridge width of 3µm, a device length of 1000µm and a single QW of 4nm with indium concentration of (0.3). The QW schematic illustrates the confinement energies as determined by the single bound electron and multiple bound heavy hole states in relation to the conduction and valence bands. For this device the only allowed optical transition is the e_1hh_1 transition resulting in a recombination wavelength at 1.119µm. Figure 1(b) is the modal gain spectrum as a function of increasing drive (pump) current from10-50mA. A peak is observed at 1.11eV corresponding to the e_1hh_1 transition. The gain spectrum curves become increasing more closely packed as the current increases. This is

attributed to the increasingly dominant Auger recombination with increasing carrier density within the QW. The 4nm SQW delivers a reasonable modal spectral gain across a relatively wide bandwidth 130nm at -3dB down from the modal gain peak at a drive current of 50mA. Figure 1(c) is the plot of ASE vs wavelength for increasing drive current 10-50mA for device A. At a drive current of 50mA the -3dB line width of the ASE spectrum is 35nm wide and is significantly narrower than the gain spectrum due to ASE being an exponential function of gain and spontaneous emission.

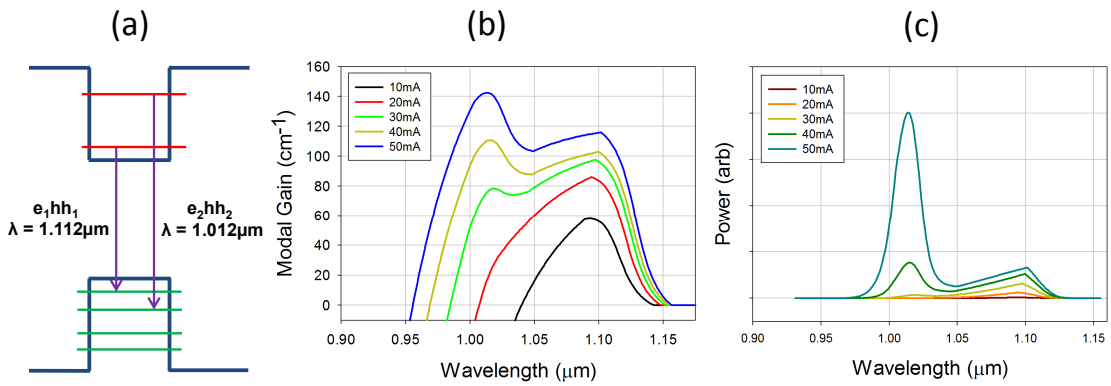

Figure 2 (a) band structure schematic of 10nm $In_{(0.3)}Ga_{(0.7)}As/GaAs$ SQW device, (b) 10nm SQW device modal gain plot, (c) 10nm SQW device ASE power curve

A method to enhance the -3db bandwidth of an SLD is to harness the emissions from higher order states [11]. Figure 2(a) shows the schematic of the band structure of a 10nm $In_{(0.3)}Ga_{(0.7)}As/GaAs$ SQW device (termed device B) designed to produce a bandwidth of 100nm centred at 1060nm by harnessing higher order transitions in the QW. The QW schematic illustrates the confinement energies as determined by the two bound electron states and multiple bound heavy hole states in relation to the conduction and valence bands. For this device there are two allowed optical transitions, e_1hh_1 transition resulting in a recombination wavelength at 1.112μm and e_2hh_2 transition resulting in a recombination wavelength at 1.012μm. Figure 1(b) plots the modal gain spectrum as a function of current (10-50mA). The gain spectrum shows a peak at 1.102μm due to e_1hh_1, and an additional peak at 1.112μm due to the e_2hh_2 transition. It is observed that the modal gain profile is now much wider as compared to device A. At a drive current of 50mA device A delivers a gain spectrum of 130nm wide at -3db down from its modal gain peak whereas device B delivers an even wider gain spectrum of 151nm at -3dB down from its modal gain peak.

Figure 1(c) is the plot of ASE vs wavelength for increasing drive current 10-50mA for device B. At a drive current of 50mA, figure 1(c) shows a large ASE power peak at 1.012μm from the e_2hh_2 recombination and a much smaller e_1hh_1 peak at 1.112μm. Whilst ASE power is successfully obtained from the e_2hh_2 transition a significant dip is observed which is detrimental for operation of device B as an SLD in OCT applications due to the generation of side lobes in the point spread function [12]. Typically, no greater than a 3dB modulation in SLD output power is considered acceptable for OCT applications. The origin of the dip in ASE is attributed to the strong modulation in the gain spectrum, which strongly influences the ASE power as it is a convolution of gain and spontaneous emission spectrum.

One possible solution in reducing the ASE spectral modulation would be to make the state separation smaller (by modifying the well width and indium composition) but this approach reduces the 3dB bandwidth of the device, and does not allow us to meet our 100nm bandwidth requirement and would shift the wavelength centre of the device spectrum from our target of 1060nm.

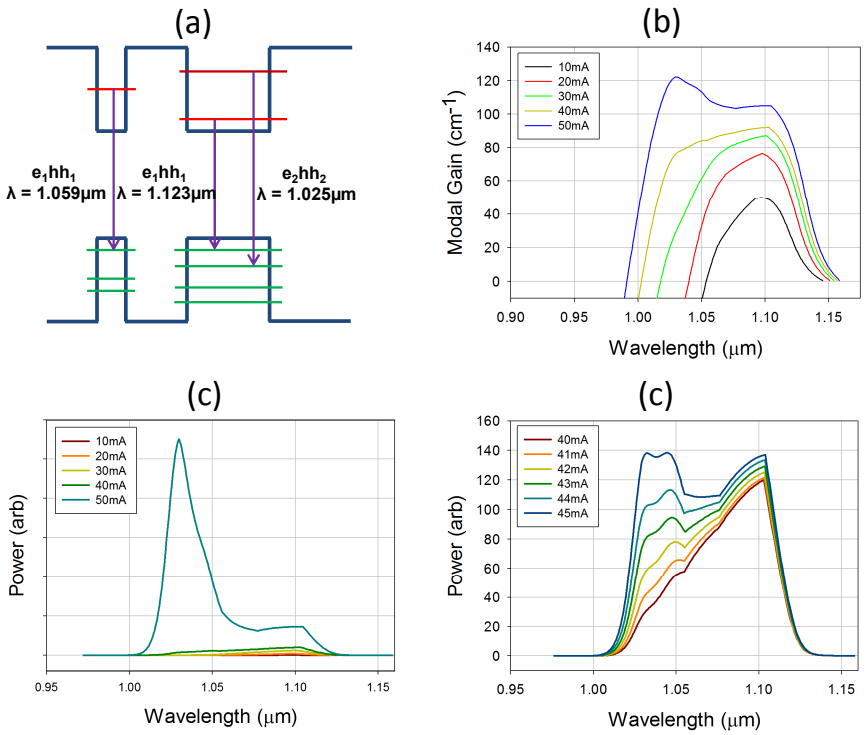

Figure 3(a) band structure schematic of combined 4nm $In_{(0.3)}Ga_{(0.7)}As/GaAs$ & 10nm $In_{(0.3)}Ga_{(0.7)}As/GaAs$ DQW device, (b) 4nm & 10nm DQW device modal gain plot, (c) 4nm & 10nm DQW device ASE power curve

One solution is to introduce a 2nd QW with an optical transition with energy mid-way between the e_1hh_1 and e_2hh_2 transition of the original QW. Figure 3(a) shows the schematic of the band structure of a 4nm $In_{(0.3)}Ga_{(0.7)}As/GaAs$ and a 10nm $In_{(0.3)}Ga_{(0.7)}As/GaAs$ forming a DQW device (termed device C) with the 4nm well on the p side of the device and the 10nm well on the n side device. We maintain the aim of producing a bandwidth of 100nm centred at 1060nm. The QW schematic shows the confinement energies and transitions from both wells. The two bound electron states and multiple bound heavy hole states in the 10nm QW and the single bound electron state in the 4nm QW are shown in relation to the conduction and valence bands. There are two allowed 10nm well transitions, e_1hh_1 gives a recombination wavelength at 1.112µm and e_2hh_2 transition gives a recombination wavelength at 1.012µm whilst the single bound electron state in the 4nm well gives a e_1hh_1 transition at 1.119µm. Figure 3(b) is the modal gain spectrum as a function of current for this DQW device and clearly shows a double gain peak at 1.102µm and at 1.112µm generated by the 10nm well. It will be noted that whilst there is a small contribution from the 4nm well the modal gain spectral profile is flatter but narrower across the plateau of the gain curve At a drive current of 50mA device B delivers a gain spectrum 151nm wide at -3db of peak gain whereas device C delivers a narrower gain spectrum of 124nm at -3dB of peak gain. In summary the modal gain spectrum is flatter but with a narrower bandwidth. Figure 3(c) shows the plot of the ASE power of the device at drive currents of 10-50mA. The additional well has resulted in a flatter ASE profile due to the flatter gain spectrum. Figure 3(d) plot shows clearly that the dominant peak changes from at ~45mA e_1hh_1 to e_2hh_2. To summarise, device C, with its ASE spectrum exhibiting less of a dip would suggest that this device is more highly suited to OCT applications but we note that the reduced gain bandwidth warrants further investigation.

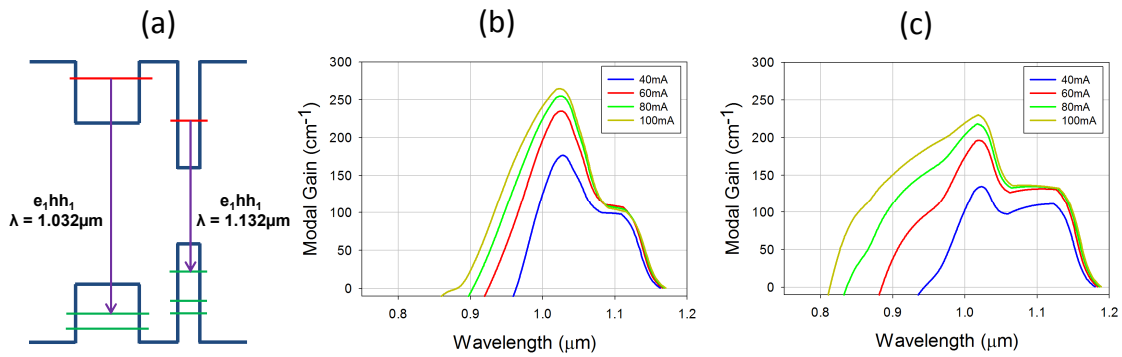

Figure 4(a) band structure schematic of unequal well combined 10nm $In_{(0.2)}Ga_{(0.8)}As/GaAs$ & 4nm $In_{(0.4)}Ga_{(0.6)}As/GaAs$ DQW device, (b) 4nm & 10nm DQW device modal gain plot, (c) 4nm & 10nm DQW device ASE power curve

Figure 4(a) shows the schematic of the band structure of a DQW device where the depth of the wells has been engineered so that the roles of the two QW's have been reversed with regard to generation and amplification of light (termed device D). The 10nm $In_{(0.2)}Ga_{(0.8)}As/GaAs$ well has been designed to generate light at a shorter wavelength of 1.032µm and the 4nm $In_{(0.4)}Ga_{(0.6)}As/GaAs$ well has been designed to generate light at the longer wavelength of 1.132µm. The 10nm well now has only one bound electron state so there is only one optical transition (e_1hh_1) from this well. Additionally the physical position of the wells has been swapped so that the 10nm well is now on the p-side of the device structure. This was observed to provide a broader gain spectrum than the inverted structure (10nm on n-side). The role of quantum well position and carrier transport will be discussed in a subsequent paper. In order to further explore the gain spectra at higher carrier densities, the device length was reduced to 500µm in order to raise the lasing threshold of the device. Figure 4(b) plots the gain spectrum for device C and 4(c) is the gain spectrum for device D with "role reversed" wells. It can be seen that there is a marked increase to the modal gain spectrum at shorter wavelengths. For example, at a wavelength of 0.9µm device C has a gain of 22.7 cm^{-1} whereas device D has a gain of 149.5 cm^{-1}.

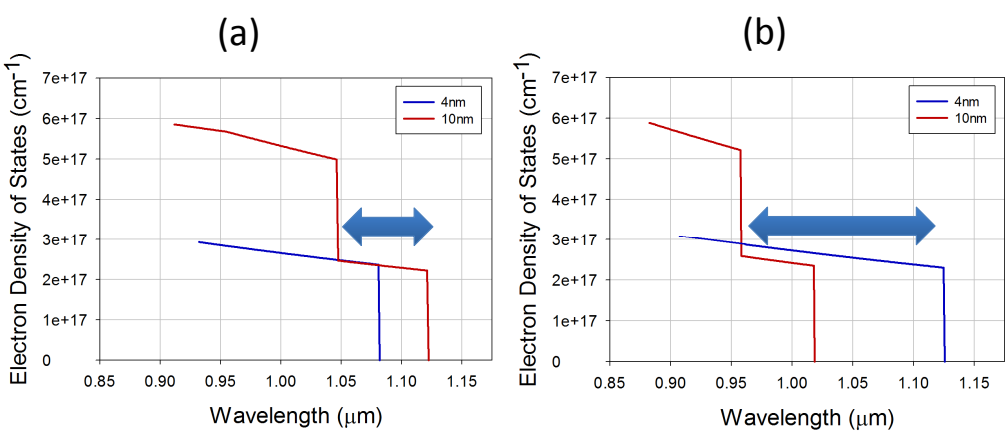

Figure 5(a) Density of states for device C, (b) density of states for device D

Figure 5 plots the density of states (DoS) as a function of wavelength for (a) device C, and (b) device D in order to illustrate the benefits of choosing role reversed MQW devices. In operation, the DoS at longer wavelengths provides a

measure of the saturated gain possible from that particular state. For wavelengths significantly shorter the DoS indicates the magnitude of absorption from that state. In order to achieve a broad gain spectrum, the states will be filled from low to high energy as current (carrier density) is increased. Additional states (e.g. due to higher order transitions) are therefore un-desirable in obtaining broad gain bandwidths at modest (i.e. manageable in terms of thermal effects, reliability, etc.) currents. In moving the e_2hh_2 transition state to shorter wavelengths in device D compared to device C it is possible to reduce the total number of states to be filled for a given gain bandwidth and enhance the bandwidth as shown in Fig 4.

3. **Summary**

We have briefly outlined the requirements of OCT in terms of broad band semiconductor devices. For the different embodiments of OCT, SOA's and SLD's are required. The operation of an SOA is known to be dominated by the gain spectrum whilst for an SLD the output power spectrum is governed by a convolution of gain and spontaneous emission spectrum. We have explored a range of single and double QW structures. We confirmed that using higher order states broadens the gain spectrum. Attempting to achieve broad band SLD's can result in significant undesirable spectral modulation. We show that this SLD spectral modulation can be ameliorated by introducing an additional well for which the lowest energy optical transition is centred on the spectral dip. Having noted a reduction in gain spectrum width we explored "role reversal" QW's where the narrow QW has a high Indium concentration to achieve long wavelength emission. This results in a modification to the DoS which is beneficial to obtaining broad bandwidth gain for a given current density.

References

[1] David Huang, Eric A Swanson, Charles P Lin, Joel S Schuman, William G Stinson, Warren Chang, Michael R Hee, Thomas Flotte, Kenton Gregory, Carmen A Puliafito, James G Fulimoto, "Optical Coherence Tomography", Science, New Series, Vol. 254, No. 5035 (Nov. 22, 1991), 1178-1181

[2] Pearse A Keane, Humberto Ruiz-Garcia, Srinivas R Sadda, "Clinical Application of Long-Wavelength (1000-nm) Optical Coherence Tomography" Opthalmic Surgery, Lasers & Imaging Vol. 42, No. 4 (Suppl), 2011

[3] Sebastian Marschall, Christian Pedersen, Peter E. Andersen, "Investigation of the impact of water absorption on retinal OCT imaging in the 1060nm range," 2012 Optical Society of America OCIS codes: (170.4500) Optical coherence tomography; (170.4460) Ophthalmic optics and devices; (350.5730) Resolution.

[4] A F Fercher, W Drexler, C K Hitzenberger, T Lasser, "Optical Coherence Tomography – Principles and Applications," Institute of Physics Publishing Rep. Prog. Phys. 66 (2003) 239-303

[5] R Leitgeb, C K Hitzenberger, A F Fercher, "Performance of Fourier domain vs time domain optical coherence tomography," Optical Society of America (2003) OCIS codes: (110.4500) Optical Coherence Tomography. (120.3890) Medical Optics Instrumentation

[6] Benjamin R Biedermann, Wolfgang Wieser, Christoph M Wigenwillig, Thomas Klein, Robert Huber, "Dispersion, coherence and noise of Fourier domain mode locked lasers," Optical Society of America 8 June 2009/ Vol. 17, No. 12 / Optics Express 9947

[7] T P Lee, Charles A Burrus Jr, B I Miller, "A Stripe-Geometry Double-Heterostructure-Amplified-Spontaneous-Emission Superluminescent Diode," IEEE J. Quant. Electron, 9(8), August 1974

[8] LaserMOD a commercially available device simulation package developed by RSOFT Design Group Inc,400 Executive Boulevard, Ste. 100, Ossining, NY 10562, USA

[9] P M Mensz, Z S Li, "Comparison of k.p Models For Quantum Well Optoelectronic Devices," Numerical Simulation of Optoelectronic Devices, 2005. NUSOD '05. Proceedings of 5th Internations Conference (19-22 Sept 2005) DOI: 10.1109/NUSOD.2005.1518142 ISBN: 0-7803-9149-7 IEEE

[10] Z Y Zhang, I J Luxmoore, C Y Jin, Q Jiang, K M Groom, D T Childs, M Hopkinson, A G Cullis, R A Hogg, "Effects of Facet Angle on Effective Facet Reflectivity and Operating Characteristics of Quantum Dot Edge Emitting Lasers and Superluminescent Light-Emitting Diodes" Aap. Phys. Lett 91, 081112 (2007)

[11] T R Chen, L Eng, Y H Zhuang, A Yariv, "Quantum Well Superluminescent Diode With Very Wide Emission Spectrum," Appl. Phys. Lett. 56 (14), 2 April 1990 American Institute of Physics 1345

[12] Thomas Klein, Wolfgang Wieser, Christoph M Eigenwillig, Benjamin R Biedermann, Robert Huber, "Megahertz OCT for ultrawide-field retinal imaging with a 1050nm Fourier domain mode-locked laser" Optical Society of America 14 February 2011 / Vol. 19, No. 4 / Optics Express 3044